Soft Matter

PAPER

A single step assembly of uniform microparticles for controlled release applications†

Wenjie Liu,[a] **Winston Wu,**[a] **Cordelia Selomulya**[*a] **and Xiao Dong Chen**[ab]

Microparticles with homogeneous properties are crucial for pharmaceutical applications where the prior knowledge of exact drug loading and release behaviour is essential to achieve targeted therapeutic goals. Various methods such as membrane microemulsion or templating to assemble uniform particles often involve multiple steps, including post-processing for purification and recovery, with additional chemical reactivity is often required to form solid particles, rendering less flexibility in the procedure. Spray drying is a common method to produce pharmaceutical particles, although control over the particle properties poses a challenge. Here we used a specially designed dryer utilising a micro-fluidic-aerosol-nozzle to atomize monodisperse droplets from a range of precursors, to generate uniform microparticles for controlled release applications. The versatility of the device enabled microparticles with easily tunable drug release kinetics to be assembled by adjusting the drying conditions or the composition of the precursors, including the use of dopants or different solvents. Significant adjustment of the release profiles could be realized by manipulating the microstructure of the microparticles. Due to the homogeneity of the particles, a direct correlation between the microstructural properties and release mechanisms could be obtained, the knowledge of which is crucial for the design of spray-dried polymeric-based pharmaceutical particles.

Introduction

Particulate-based carriers in micro- and nano-scale play important roles in therapeutic and diagnostic applications,[1,2] due to the potential benefits such as increased bioavailability, reduced risk of systemic toxicity, and low probability of causing local irritation in comparison to conventional (monolithic) formulations. When used in the oral dosage form, particulates are less affected by gastric emptying, reducing the variation in gastrointestinal transit time.[3] At the same time, behaviors such as degradation, uptake, and clearance of particulates are closely related to their size and shape.[4–6] Thus, polydisperse particles might induce irreproducible release behavior with varying functionalities.[6]

There are several approaches to fabricate uniform particles, including membrane emulsification,[7] hydrogel template,[8] acoustic excitation,[9] and electrospraying.[6,10] Often these methods involve intricate steps and long operation time before obtaining the final formulation.[11] Post-processing such as the washing and purification stages also lead to low loading efficiency that is

highly undesirable for expensive therapeutic agents. These issues restrict the feasibility for clinical trials or large scale production.[11] Thus there is an urgent need for a robust process to produce uniform microparticles with controllable functionalities.[12]

Here we demonstrated the preparation of uniform microparticles *via* a modified spray drying technique. Spray drying is ideal to form particles in a single step, with feasibility for large-scale production, and applicability for both hydrophilic and hydrophobic materials. It does not require further washing steps, while any harsh chemical reactions for particle solidification can be avoided.[11,13] The inherent drawback for conventional spray drying is that the atomizers generally produce polydisperse droplets with different sizes and trajectories. These droplets then experience various drying profiles within the same environment, resulting in poor reproducibility over particle properties and functionalities from batch-to-batch operation (or even from the same batch). We have previously reported the methodology to produce photoluminescent microcomposites, by ensuring identical drying experience for every individual droplet into solid particles.[14] Here we used the same versatile approach to fabricate microparticles with uniform properties for controlled drug release applications. The novelty of this study lies in the ability to directly manipulate the microstructure of the polymeric microparticles to control the drug release mechanisms, made possible by the capability to generate uniform microparticles in a single

a Department of Chemical Engineering, Monash University, Clayton, VIC, 3800, Australia. E-mail: cordelia.selomulya@monash.edu; Fax: 61 3 99055686; Tel: 61 3 99053436

b Department of Chemical and Biochemical Engineering, Xiamen University, 361005 Fujian Province, P.R. China

step from a relatively complex range of precursors. Polymeric aqueous dispersion is employed as the basic excipient for particle formulation, which offers advantages including (1) the extra flexibility of the polymer state that can be tuned from the solvent composition and (2) the possibility to eliminate the use of organic solvents. Eudragit® RS 30D is used as a model polymer dispersion with the chemical structure shown in Fig. 1, schematically representing their physicochemical behaviors in different solvent systems.[15,16] Vitamin B$_{12}$ is used as a hydrophilic model drug to test the controlled release properties of the microparticles with distinct microstructures.

Experimental section

Materials

Eudragit® RS 30D (30% aqueous dispersion) was kindly provided by Evonik Degussa Industries (Australia). Vitamin B$_{12}$ (VB$_{12}$), chitosan (low molecular weight) and tetraethoxysilane (TEOS) were purchased from Sigma-Aldrich (Australia). Acetone and absolute ethanol were of analytical grade from Merck (Australia). All other reagents used were of analytical grade. Deionized water (Milli-Q) was used for all precursor preparation.

Precursor preparation

The precursors for spray drying were prepared by directly dispersing Eudragit® RS 30D into certain solvents. To investigate the effects of solvents and dopants, different formulations of precursors were prepared (Table 1). Calculated amounts of chitosan and TEOS were added to reach 0.5% (w/v). The total mass content of excipients was set to be 3% (w/v). The dissolution of chitosan and hydrolysis of TEOS were facilitated in an acidic medium. Certain amount of VB$_{12}$ was added with drug: excipients ratio of 5%.
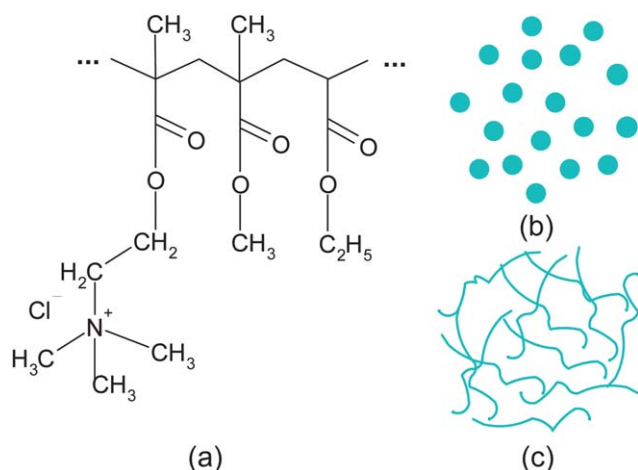
Fig. 1 (a) Chemical structure of Eudragit® RS; Eudragit® RS, which is insoluble in water but dissolves in organic solvents, has different physicochemical behaviors within different solvents: (b) exists as polymeric nano-dispersions in aqueous medium, (c) exists as polymer solutions in organic solvents.

Microparticles fabrication

Monodisperse droplets were generated from precursor solution by a micro-fluidic aerosol nozzle system, with an orifice diameter of 75 μm. Briefly, the precursor solutions were fed into a standard steel reservoir and dehumidified instrument air was used to force the liquid in the reservoir to jet through the nozzle. The liquid jet was broken into droplets by disturbance from vibrating piezoceramics. The droplet formation mode was monitored by a digital SLR camera (Nikon, D90) with a speed-light (Nikon SB-400) and a micro-lens (AF Micro-Nikkor 60mm f/2.8D). The liquid flow rate and applied disturbance frequency were adjusted to best achieve monodisperse droplet formation.[17] These monodisperse droplets obtained were well dispersed and dried at a specific drying temperature (ESI†, Fig. S1). In a typical experiment, the drying temperature of 180 °C was used. Temperatures of 130 °C and 155 °C were also set to investigate the influence of drying temperature on microparticle characteristics and drug release behaviors.

Particle characterization

Images of microparticles were recorded by light microscopy (Motic B1-223A, UK). Particle size and size distribution were analyzed using the software package Motic Images Plus 2.0 ML and ImageJ. The average particle size ($\bar{d}$) was defined as $\bar{d} = \sum_{i=1}^{n} \frac{d_i}{N}$ and the span of size distribution was described as span $= \frac{(d_{90} - d_{10})}{d_{50}}$, where d_i was the diameter of the i-th particle, N was the total number of particles counted, d_{90}, d_{50}, d_{10} were the cumulative particle sizes at 90%, 50%, and 10%, respectively. The morphology and structure of microparticles before and after the drug release test were characterized by field-emission scanning electron microscopy (FESEM, JEOL 7001F, Japan). FT-IR spectrum was performed on a Perkin Elmer spectrometer in the wavelength range of 4000–400 cm^{-1}, at a spectral resolution of 4 cm^{-1}. Differential scanning calorimetry (DSC) was determined with a TA-Q100 DSC. The DSC tests were conducted over a temperature range from 0 to 150 °C at 10 °C min^{-1} under a dry nitrogen flow (50 mL min^{-1}).

In vitro drug release test

In a typical experiment, the drug-loaded microparticles (50 mg) were weighted into 100 mL conical flask, and 50 mL of PBS (phosphate buffer solution) release medium (pH 7.4) was transferred into the flask. Due to the solubility of chitosan at acidic condition, the release test for microparticles containing chitosan was also conducted at pH 1.2 using HCl solution. The flask was kept in a shaking incubator at 37 °C with constant agitation (100 rpm) for the duration of the release test (28 hours). At certain time intervals, 1 mL of the release medium was withdrawn from the flask and replaced with the same amount of fresh release medium. Collected samples were transferred into 1.7 mL microtubes, centrifuged for 5 min at 10 000 rpm (Heal force, Neofuge 23R) and subjected to assay immediately. The content of VB$_{12}$ in the sample was determined by a microplate reader (SpectraMax M2e, Molecular devices) at the wavelength of

Table 1 Formulations of precursors for spray drying

Formulation no.	Eudragit® RS[a] (w/v)	Solvent composition[b]	Chitosan (w/v)	TEOS (w/v)	Vitamin B$_{12}$ (w/w)	Vitamin B$_{12}$ loading (%)
R$_3$(H)	3%	H	—	—	5%	97.10 ± 1.09
R$_3$(H$_1$A$_2$)	3%	H : A = 1 : 2	—	—	5%	96.01 ± 0.95
R$_3$(H$_1$A$_2$E$_{0.5}$)	3%	H : A : E = 1 : 2 : 0.5	—	—	5%	97.27 ± 1.18
R$_{2.5}$C$_{0.5}$(H)	2.5%	H	0.5%	—	5%	97.28 ± 1.95
R$_{2.5}$T$_{0.5}$(H)	2.5%	H	—	0.5%	5%	96.15 ± 2.79

[a] *e.g.* 10 mL Eudragit® RS 30D was added into 90 mL deionized water to get a 3% (w/v) Eudragit® RS precursor. [b] H, A, and E were short for H$_2$O, acetone, and ethanol. All ratios are expressed in volume.

maximum absorbance (361 nm). Each sample was performed in triplicate.

The total amount of VB$_{12}$ loaded into microparticles was determined by dissolving an accurately weighed amount of microparticles in 1 mL ethanol (or mixture of ethanol and acidic acid/NaOH solution for R$_{2.5}$C$_{0.5}$(H) and R$_{2.5}$T$_{0.5}$(H) particles, respectively). After the dissolution of particles, the solutions were centrifuged for 5 min at 10 000 rpm and the amount of VB$_{12}$ in supernatant was determined by the microplate reader under 361 nm. The loading efficiency of VB$_{12}$ was calculated by dividing the amount of drug in the microparticles by the initial amount of drug added.

## Results and discussion

Fabrication of uniform microparticles

The quality of the initial droplets was a prerequisite to obtain homogenous microparticles.[18] Fig. S2 (ESI†) showed the photographs of the droplets generation process, indicating the uniformity of the initial droplets. The size and morphology of spray-dried microparticles were also confirmed by SEM images (Fig. 2 and 3). The particle size distributions were summarized in Fig. 4, revealing narrow size distributions for all samples. The homogenous properties suggested that every individual droplet experienced a similar drying process in the dryer chamber, so that any added drugs in the precursors would be incorporated equally into each microparticle of the same size and morphology.[19] The drug loading efficiency for each sample was summarized in Table 1, indicating the high (close to 100%) drug loading of spray-dried microparticles. The loading efficiency was significantly higher than those attainable with wet chemistry-based methods (typically with loading efficiency of less than 50%),[8,20] due to losses of encapsulated ingredients during the washing steps.

Particle morphology

All microparticles obtained in this study generally exhibited pot-like shapes (round or wrinkled). The SEM photographs of R$_3$(H) (Fig. 2) showed that the microparticles were pot-like with relatively smooth surface. The hollow structure was confirmed by SEM image (ESI†, Fig. S3). Microparticles obtained from different drying temperature displayed similar morphology, indicating that the drying temperature (in the range investigated here) had little effect on the shapes of spray-dried microparticles.

Under the same operating conditions, different shaped microparticles were observed when different types of solvent were used (Fig. 2, 3A and B). In particular, by changing the composition of solvent from H$_2$O (100%) to a mixture of H$_2$O and acetone with a ratio of 1 : 2, the shape was significantly deformed with the wrinkling of the particle surface. This was due to the difference in boiling points and specific heat capacities of the different solvents, which induced different latent heat of evaporation and drying rates. A faster drying rate resulted in shorter drying time and more extreme drying behavior (*i.e.* faster heat and mass transfers). Thus the tendency to deform for these droplets was increased during the more vigorous drying process.[21,22] The boiling points and specific heat capacities of solvents were in the following order: H$_2$O > ethanol > acetone. As expected, the deformation of microparticles was most notable for R$_3$(H$_1$A$_2$) which contained the highest amount of acetone.
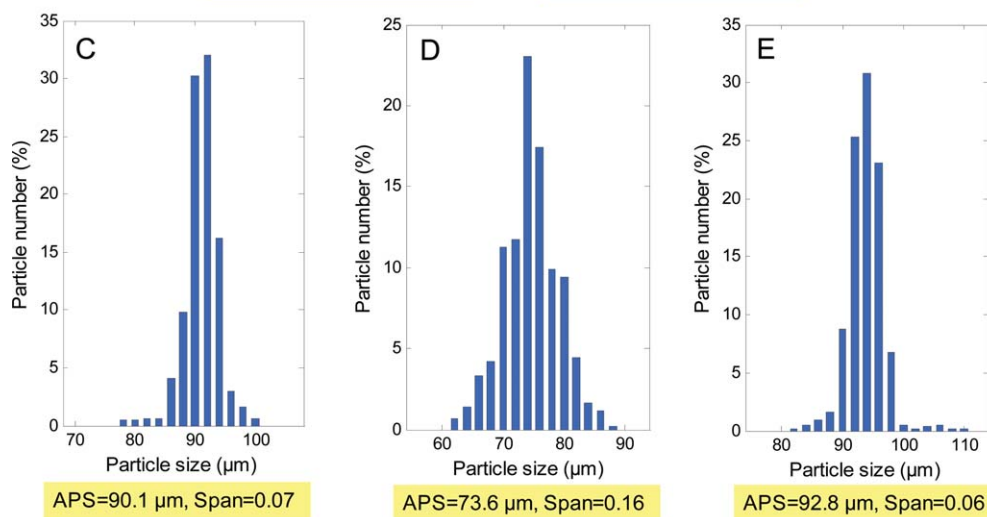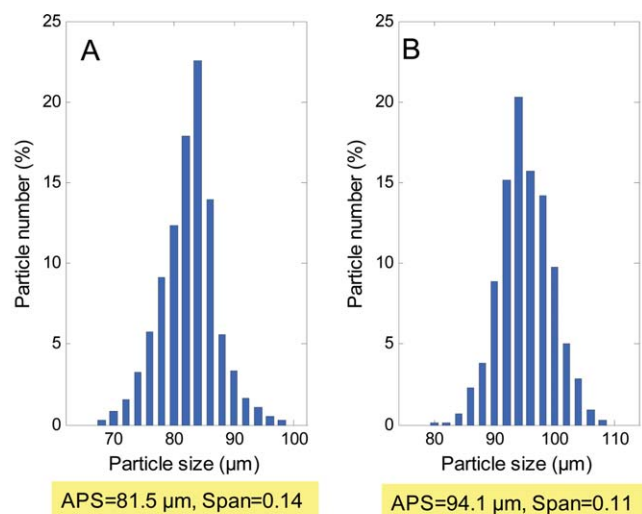
Fig. 3C and D illustrated that different dopants could also affect particle morphology. The round pot-shape was significantly deformed with surface roughness enhanced when 0.5% chitosan was incorporated. With the addition of 0.5% TEOS, the particle shape was changed into a bowl-like morphology with a large singular opening on the surface. It has been previously reported that the morphology of spray-dried microparticles was strongly dependent on the raw materials.[1,22] Here we also demonstrated this phenomenon by spray drying precursors containing only 1% chitosan or 1% TEOS (Fig. 5) that showed
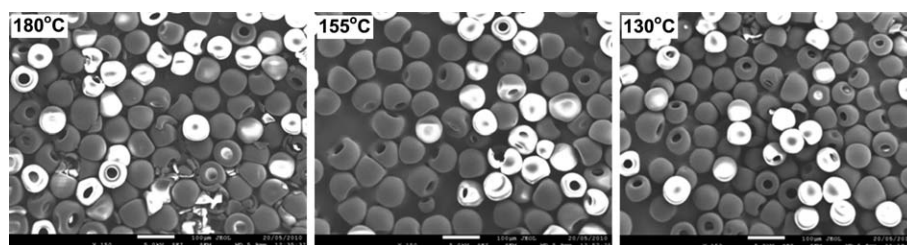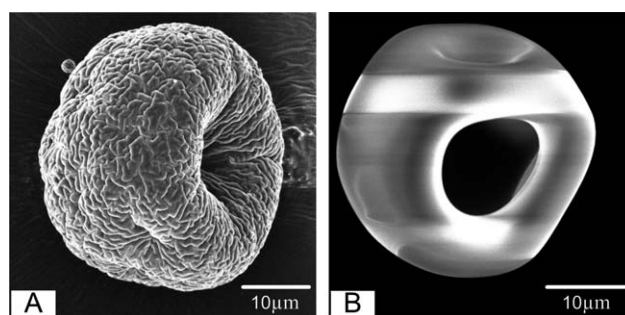

Fig. 2 SEM photographs of R$_3$(H) microparticles fabricated at different temperatures. (Scale bar: 100 μm.)
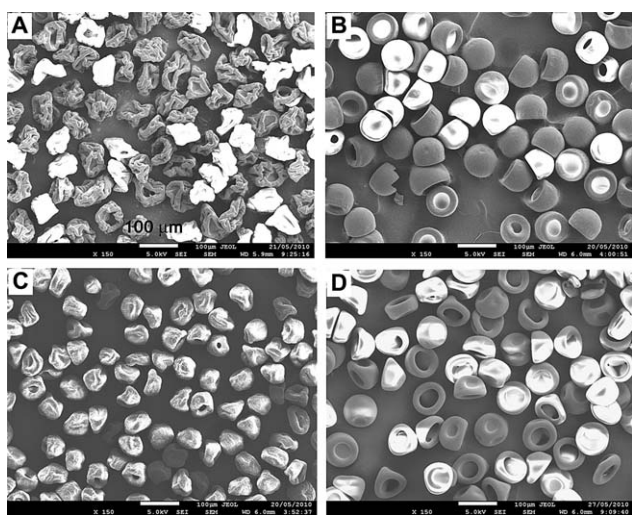
Fig. 3 SEM photographs of the spray-dried microparticles: (A) $R_3(H_1A_2)$, (B) $R_3(H_1A_2E_{0.5})$, (C) $R_{2.5}C_{0.5}(H)$ and (D) $R_{2.5}T_{0.5}(H)$. (Scale bar: 100 μm.)

Fig. 5 SEM photographs of spray-dried microparticles of (A) 1% chitosan and (B) 1% TEOS.

distinctive surface textures and particle shapes. The morphologies obtained for $R_{2.5}C_{0.5}(H)$ and $R_{2.5}T_{0.5}(H)$ (Fig. 3C and D) simply confirmed these effects of dopant addition (rough and smooth textures from chitosan and TEOS, respectively) on the resulting microparticles.
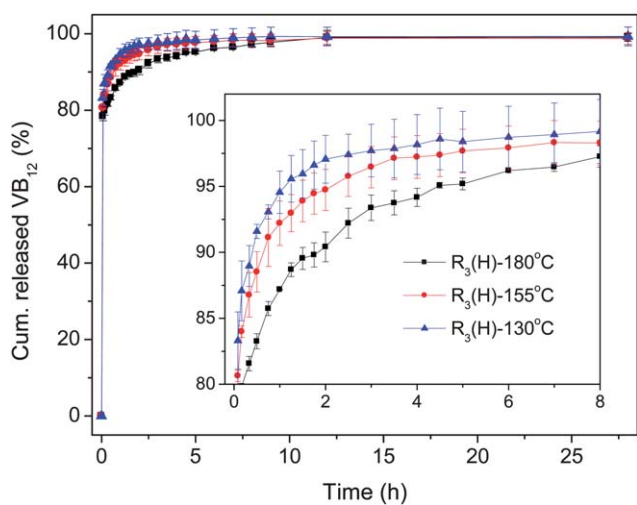

Fig. 4 Size distributions of the spray-dried microparticles (APS: average particle size): (A) $R_3(H)$, (B) $R_3(H_1A_2)$, (C) $R_3(H_1A_2E_{0.5})$, (D) $R_{2.5}C_{0.5}(H)$ and (E) $R_{2.5}T_{0.5}(H)$.

Fig. 6 Cumulative *in vitro* release of VB_{12} from the spray-dried microparticles fabricated at different temperatures (inset showing release data at initial time period).

Effects of drying temperature

The release profiles of VB_{12} from $R_3(H)$ microparticles fabricated at different drying temperatures are shown in Fig. 6. The drug release rate was slightly accelerated with the lower drying temperature. The moisture contents of microparticles spray dried at 180 °C, 155 °C, and 130 °C were $4.32 \pm 0.13\%$, $4.94 \pm 0.13\%$, and $5.35 \pm 0.14\%$, respectively. Given the same particle composition and particle size, the different drug release rates could be ascribed to different moisture contents of the microparticles. An increasing hydrophilic domain at higher moisture content enhanced the permeability of microparticles, thus facilitating buffer penetration and faster drug release rate.[23,24]

After the initial burst release, the remaining drug was released more evenly with the release rate decreasing with time. At the initial release stage, the more rapid drug release was due to the polymer water uptake and swelling accompanied by drug diffusion as reported before.[25] At the latter stage, drug diffusion would become the main driving force for release due to less availability of VB_{12} near the particle surface.[25]

Effects of solvent

Since Eudragit® RS has different physicochemical behaviors in aqueous and organic based solvents, the type of solvent used would have influenced the microstructures of the particles.[11,25,26] The proposed microstructures fabricated from different solvents were shown in Fig. 7A and B. Eudragit® RS, as a water insoluble polymer, existed in the form of nano-dispersion with H_2O as solvent. With partial replacement of acetone or ethanol, the polymer which was soluble in acetone or ethanol dissolved, so that the entanglement of molecular chains provided more barriers for drug diffusion.

We confirmed the effects of solvent type by comparing the release data for $R_3(H)$, $R_3(H_1A_2)$, and $R_3(H_1A_2E_{0.5})$ (Fig. 8). Microparticles using water as solvent ($R_3(H)$) released 80% of total VB_{12} in 0.5 h and almost 100% within 5 h. With the incorporation of acetone or ethanol, the initial burst effect and
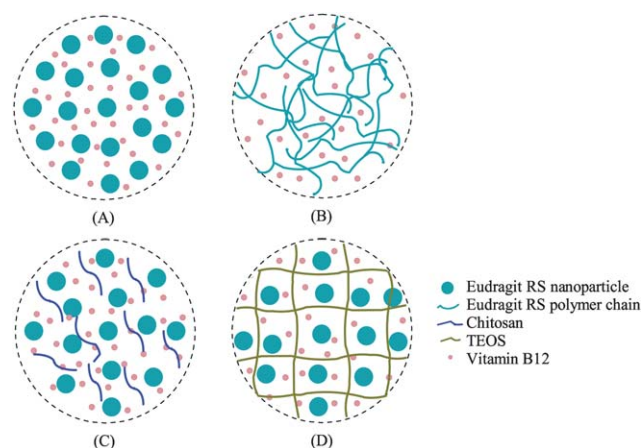

Fig. 7 Schematic diagrams of the microstructure of spray-dried microparticles: (A) $R_3(H)$, (B) $R_3(H_1A_2)$ and $R_3(H_1A_2E_{0.5})$, (C) $R_{2.5}C_{0.5}(H)$ and (D) $R_{2.5}T_{0.5}(H)$.

the subsequent release rate were effectively decelerated. As the particles were fabricated under the same drying condition with equal amount of VB_{12} and Eudragit® RS polymer, the different drug release profiles could only be attributed to the difference in the physical state of the polymer due to the solvent and/or the spatial distribution of VB_{12}, as discussed in the latter section.

We also observed the morphology and surface texture of these particles after the release test. Fig. 9 showed the morphology of the original spray-dried microparticles (Fig. $9A_0$–C_0), and after the release test (Fig. $9A_1$–C_1). There was no significant change in the morphology of microparticles before and after drug release for $R_3(H_1A_2)$ and $R_3(H_1A_2E_{0.5})$. However, small pores emerged in $R_3(H)$ microparticles after the release of VB_{12} (Fig. $9A_1$). The existence of pores after the release test also confirmed the packing structure for $R_3(H)$ as proposed in Fig. 7A.

To confirm the hypothesis of the different physical states of Eudragit® RS for $R_3(H)$, $R_3(H_1A_2)$, and $R_3(H_1A_2E_{0.5})$, the thermal properties of microparticles were analyzed with DSC. The results from DSC test (Fig. 10) showed that the curves
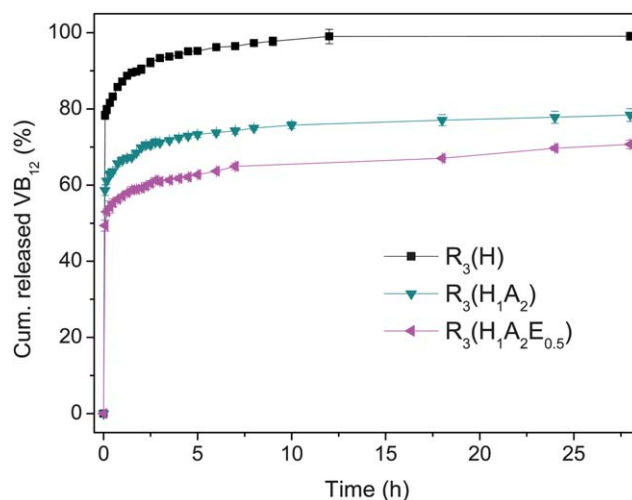
Fig. 8 Cumulative *in vitro* release of VB_{12} from the spray-dried microparticles fabricated from different solvents.
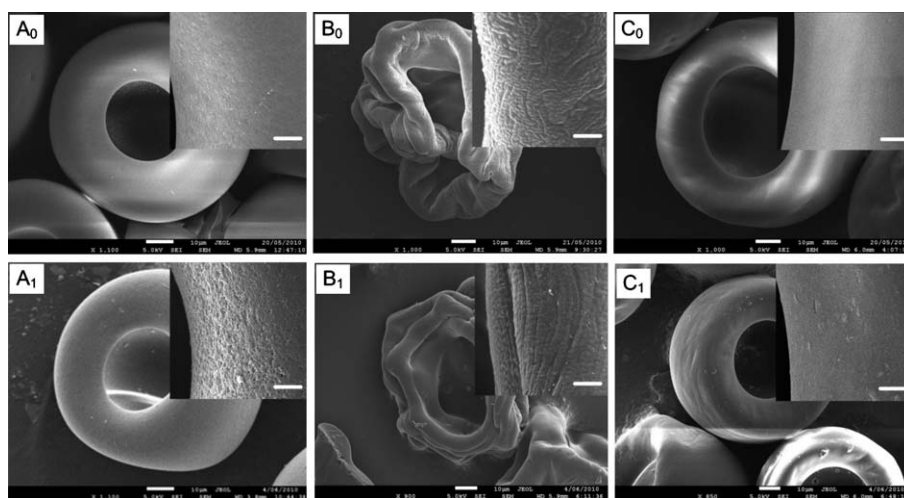
Fig. 9 SEM photographs of the spray-dried microparticles fabricated from different solvents before (A_0, B_0, C_0) and after (A_1, B_1, C_1) drug release test: (A) $R_3(H)$, (B) $R_3(H_1A_2)$, (C) $R_3(H_1A_2E_{0.5})$. (Scale bar of main picture: 10 μm; scale bar of inset: 2 μm.)
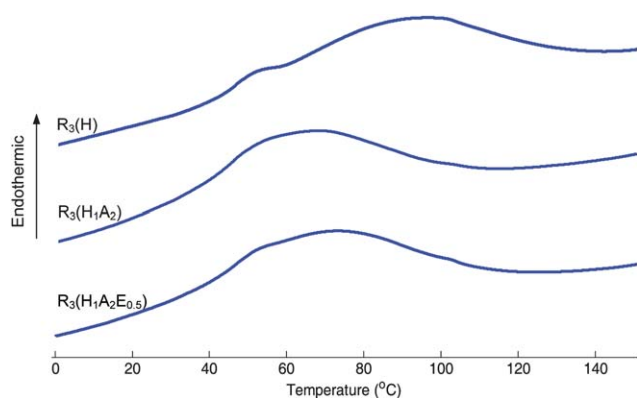
**Fig. 10** DSC curves of the drug-loaded Eudragit® RS microparticles fabricated from different solvents.

started to rise from a similar temperature, with the shapes of DSC thermograms for $R_3(H_1A_2)$ and $R_3(H_1A_2E_{0.5})$ similar to each other. The peaks around 65 °C were caused by the glass transition of Eudragit® RS.[25,27] However the peak was extended for the aqueous system of $R_3(H)$, with the maximum appearing at about 100 °C. In all three cases, the particle size was similar (about 80–90 μm). It could be concluded that the difference in DSC curves was solely due to the difference of the physical state of the polymer, namely the packing of polymeric nanoparticles in $R_3(H)$ and the polymer chains in $R_3(H_1A_2)$ and $R_3(H_1A_2E_{0.5})$.

Although the physical state of the polymer was proven to be relatively similar for $R_3(H_1A_2)$ and $R_3(H_1A_2E_{0.5})$, the drug release profiles of the microparticles were quite distinctive. To explain this phenomenon, the different particle morphologies should be considered. Fig. 9B_0 and C_0 indicated that the microparticles of $R_3(H_1A_2)$ and $R_3(H_1A_2E_{0.5})$ displayed noticeably different shapes and surface characteristics. The deformed shape and wrinkled surface of $R_3(H_1A_2)$ significantly increased the surface area for similar size particles, thus allowing more contact with the release medium. This result was consistent with previous studies which reported that particles with smoother surface displayed slower drug release characteristics.[28,29]

We also compared the FT-IR spectra of the microparticles prepared using different solvent systems (Fig. 11). No significant change was observed in the entire spectrum (thus confirming the same composition for different microparticles), with two slight deviations observed. Firstly, the two peaks around 1580 and 1625 cm^{-1} in ($R_3(H)$) almost disappeared for $R_3(H_1A_2)$ and $R_3(H_1A_2E_{0.5})$. In addition, the two peaks around 1380 and 1400 cm^{-1} for $R_3(H_1A_2)$ and $R_3(H_1A_2E_{0.5})$ combined into a single peak for ($R_3(H)$). These peaks were the characteristic peaks of VB_{12}, and the relatively higher intensity of these peaks in $R_3(H)$ indicated the higher amount of VB_{12} existing on or near the particle surface.[6,30] These data suggested that the fast initial drug release rate of $R_3(H)$ microparticles could be directly linked to the spatial distribution of VB_{12}.

Effects of dopants

The change in solvent composition has been proven to be an effective way to tune the drug release profiles. It would be ideal if the usage of organic solvents could be completely avoided, while
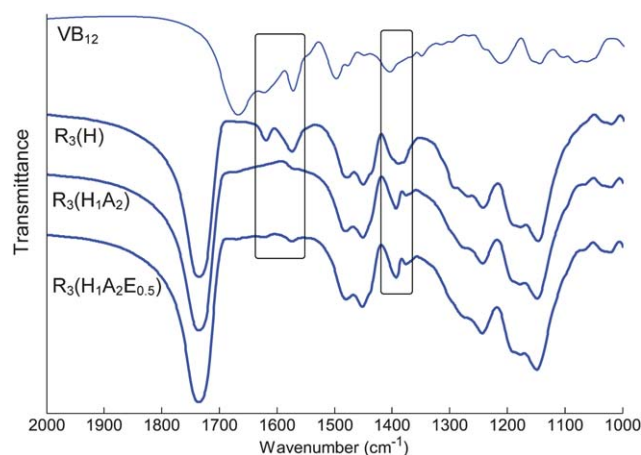
Fig. 11 FT-IR spectrum of VB_{12} and VB_{12} loaded Eudragit RS microparticles fabricated from different solvents.

still enabling the regulation of the release profiles. Complex materials consisting of blends of polymers or copolymers have been developed previously to obtain the desired functionalities of pharmaceutical particles.[31] Herein, the drug release profiles were tuned by different blending strategies of the precursors prior to drying.

To investigate the effects of incorporating a hydrophilic compound on the drug release rate, chitosan was chosen as the model polymer. The high amount of amino groups on polymer chains provided chitosan with good hydrophilic properties and solubility in acidic medium. The microstructure of the spray-dried microparticles was displayed in Fig. 7C. As shown in Fig. 12, the incorporation of chitosan effectively increased the drug release rate. Chitosan has been reported to trigger the drug release for Eudragit® RS beads and enhance the water uptake for Eudragit® RS films,[32,33] consistent with the data reported here. The characteristics of microparticles before and after drug release test at pH 7.4 were compared (Fig. 13A_0 and A_1), with no visible change observed in the particle morphology and surface characteristics. Due to the pH dependent solubility of chitosan, the release test was also performed in HCl solution (pH 1.2) to simulate gastric fluid, as the pH closest to that of a human's stomach. Because of the fast release rate for these microparticles, no noticeable distinction in the drug release rate was observed with different release media. However, distinct surface characteristic and inner structure of microparticles were observed after the release test, due to chitosan solubility in the acidic condition (ESI†, Fig. S4).

To enable drug release in a more controlled manner, a network structure would be ideal to provide increasing drug diffusion barriers. It had been reported that the acidic hydrolysis of TEOS generated a rigid interpenetrating network (as illustrated in Fig. 7D), which did not swell but could be degraded or eroded in a release medium.[34,35] As expected, the incorporation of TEOS effectively slowed down the drug release rate (Fig. 12). The drug release was completed after about 24 hours, accompanied with a relatively sustained release rate at the initial stage. In addition, the continuous degradation of silica network enhanced drug diffusion and compensated the diminished drug accessibility,
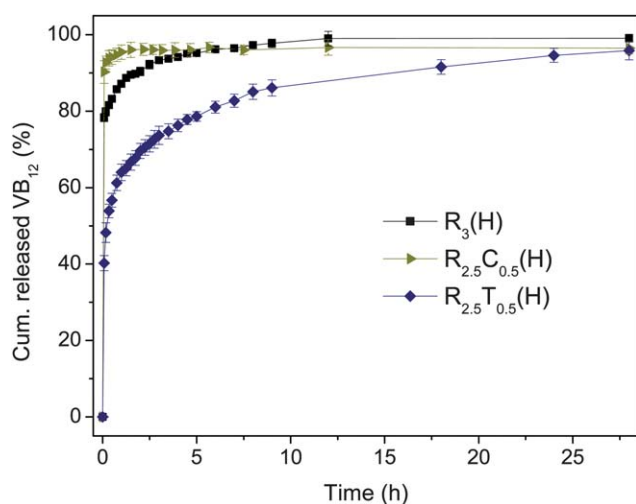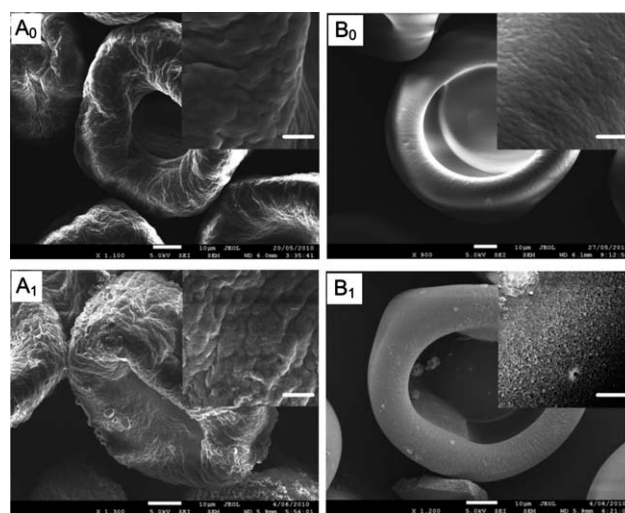

Fig. 13 SEM photographs of the spray-dried microparticles fabricated using different dopants before (A_0, B_0) and after (A_1, B_1) drug release test: (A) $R_{2.5}C_{0.5}(H)$ and (B) $R_{2.5}T_{0.5}(H)$. (Scale bar of main picture: 10 μm; scale bar of inset: 2 μm.)

with a relatively faster drug release rate achieved at the latter stage compared with the other cases. SEM photographs of the microparticles before and after the release tests clearly revealed the degradation of the silica matrix (Fig. 13B_0 and B_1).

The analysis of the release data with the empirical equation proposed by Peppas and Sahlin: $(M_t/M_\infty) = k_1 t^m + k_2 t^{2m}$ was also conducted to further explain the drug release mechanisms from the microparticles, where M_t/M_∞ was the fraction of drug released at time t, and k_1, k_2, and m were the respective constants from best fit with the experimental data[36] (ESI†, drug release kinetics).

Conclusion

The design of uniform drug carriers *via* a continuous, one-step particle formation process was demonstrated here, with understanding of the difference in physicochemical behaviors of the excipients within aqueous and organic-based solvent systems to control the drug release kinetics. The drug release rates of the carriers could be adjusted in the absence of organic solvents, by changing the drying temperature or incorporating different dopants. The microparticles obtained were uniform with almost 100% drug loading efficiency, and virtually no limitation to the range of excipients and drugs including heat sensitive materials such as polymers or proteins, due to the relatively low temperature range used. The strategy to control the release functionality of microparticles from microstructures can be applied to other materials with unique physicochemical behaviors under different conditions such as pH-sensitive or thermal sensitive materials to fabricate particles with unique microstructures and to tune the release kinetics.

Fig. 12 Cumulative *in vitro* release of VB_{12} from the spray-dried microparticles fabricated using different dopants.

References

1 J. Xie, J. C. M. Marijnissen and C.-H. Wang, *Biomaterials*, 2006, **27**, 3321–3332.
2 E. Pisani, N. Tsapis, J. Paris, V. Nicolas, L. Cattel and E. Fattal, *Langmuir*, 2006, **22**, 4397–4402.

3 N. S. Dey, S. Majumdar and M. E. B. Rao, *Trop. J. Pharm. Res.*, 2008, **7**, 1067–1075.

4 M. Dunne, O. I. Corrigan and Z. Ramtoola, *Biomaterials*, 2000, **21**, 1659–1668.

5 L. Ilium, S. S. Davis, C. G. Wilson, N. W. Thomas, M. Frier and J. G. Hardy, *Int. J. Pharm.*, 1982, **12**, 135–146.

6 Y.-H. Lee, F. Mei, M.-Y. Bai, S. Zhao and D.-R. Chen, *J. Controlled Release*, 2010, **145**, 58–65.

7 W. Wei, L. Yuan, G. Hu, L.-Y. Wang, J. Wu, X. Hu, Z.-G. Su and G.-H. Ma, *Adv. Mater.*, 2008, **20**, 2292–2296.

8 G. Acharya, C. S. Shin, M. McDermott, H. Mishra, H. Park, I. C. Kwon and K. Park, *J. Controlled Release*, 2010, **141**, 314–319.

9 C. Berkland, K. Kim and D. W. Pack, *J. Controlled Release*, 2001, **73**, 59–74.

10 M.-W. Chang, E. Stride and M. Edirisinghe, *Soft Matter*, 2009, **5**, 5029–5036.

11 B. G. De Geest, S. De Koker, Y. Gonnissen, L. J. De Cock, J. Grooten, J. P. Remon and C. Vervaet, *Soft Matter*, 2010, **6**, 305–310.

12 A. D. Dinsmore, M. F. Hsu, M. G. Nikolaides, M. Marquez, A. R. Bausch and D. A. Weitz, *Science*, 2002, **298**, 1006–1009.

13 K. Masters, *Spray Drying Handbook*, Longman Scientific and Technical, New York, 5th edn, 1991.

14 W. D. Wu, S. X. Lin and X. D. Chen, *AIChE J.*, 2010, DOI: 10.1002/aic.12364.

15 D. M. Omari, A. Sallam, A. Abd-Elbary and M. El-Samaligy, *Int. J. Pharm.*, 2004, **274**, 85–96.

16 A. San Miguel, J. Scrimgeour, J. E. Curtis and S. H. Behrens, *Soft Matter*, 2010, **6**, 3163–3166.

17 W. D. Wu, R. Amelia, N. Hao, C. Selomulya, D. Zhao, Y.-L. Chiu and X. D. Chen, *AIChE J.*, 2011, DOI: 10.1002/aic.12489.

18 W. D. Wu, K. Patel, S. Rogers and X. D. Chen, *Drying Technol.*, 2007, **25**, 1907–1916.

19 G. V. R. Rao, G. P. López, J. Bravo, H. Pham, A. K. Datye, H. F. Xu and T. L. Ward, *Adv. Mater.*, 2002, **14**, 1301–1304.

20 F. Ito, H. Fujimori and K. Makino, *Colloids Surf., B*, 2008, **61**, 25–29.

21 Y.-F. Maa, H. R. Costantino, P.-A. Nguyen and C. C. Hsu, *Pharm. Dev. Technol.*, 1997, **2**, 213–223.

22 D. E. Walton, *Drying Technol.*, 2000, **18**, 1943–1986.

23 M. G. Lara, M. V. L. B. Bentley and J. H. Collett, *Int. J. Pharm.*, 2005, **293**, 241–250.

24 F. Lecomte, J. Siepmann, M. Walther, R. J. MacRae and R. Bodmeier, *Biomacromolecules*, 2005, **6**, 2074–2083.

25 T. Kristmundsdottir, O. S. Gudmundsson and K. Ingvarsdottir, *Int. J. Pharm.*, 1996, **137**, 159–165.

26 B. Gander, H. P. Merkle, V. P. Nguyen and N.-T. Ho, *J. Phys. Chem.*, 1995, **99**, 16144–16148.

27 S.-Y. Lin and H.-L. Yu, *J. Appl. Polym. Sci.*, 2000, **78**, 829–835.

28 T. K. Mandal, *Drug Dev. Ind. Pharm.*, 1999, **25**, 773–779.

29 A. Lamprecht, H. Yamamoto, H. Takeuchi and Y. Kawashima, *J. Controlled Release*, 2003, **90**, 313–322.

30 K. S. Taraszka, E. Chen, T. Metzger and M. R. Chance, *Biochemistry*, 1991, **30**, 1222–1227.

31 N. Angelova and D. Hunkeler, *Trends Biotechnol.*, 1999, **17**, 409–421.

32 K. Kaur and K. Kim, *Int. J. Pharm.*, 2009, **366**, 140–148.

33 W.-a. Sakchai, P. Chureerat and S. Srisagul, *AAPS PharmSciTech*, 2006, **7**, Article 30.

34 S.-B. Park, J.-O. You, H.-Y. Park, S. J. Haam and W.-S. Kim, *Biomaterials*, 2001, **22**, 323–330.

35 T. Czuryszkiewicz, S. Areva, M. Honkanen and M. Lindén, *Colloids Surf., A*, 2005, **254**, 69–74.

36 N. A. Peppas and J. J. Sahlin, *Int. J. Pharm.*, 1989, **57**, 169–172.